

η' photoproduction on the proton for photon energies from 1.527 to 2.227 GeV

M. Dugger,¹ J.P. Ball,¹ P. Collins,¹ E. Pasyuk,¹ B.G. Ritchie,¹ G. Adams,³¹ P. Ambrozewicz,¹¹ E. Anciant,⁶ M. Anghinolfi,¹⁸ B. Asavapibhop,²⁴ G. Asryan,⁴⁰ G. Audit,⁶ H. Avakian,^{17,35} H. Bagdasaryan,²⁹ N. Baillie,³⁹ N.A. Baltzell,³⁴ S. Barrow,¹² V. Batourine,²² M. Battaglieri,¹⁸ K. Beard,²¹ I. Bedlinskiy,²⁰ M. Bektasoglu,^{28,29,*} M. Bellis,⁴ N. Benmouna,¹³ B.L. Berman,¹³ N. Bianchi,¹⁷ A.S. Biselli,^{31,4} B.E. Bonner,³² S. Bouchigny,^{35,19} S. Boiarinov,^{20,35} R. Bradford,⁴ D. Branford,¹⁰ W.J. Briscoe,¹³ W.K. Brooks,³⁵ S. Bültmann,²⁹ V.D. Burkert,³⁵ C. Butuceanu,³⁹ J.R. Calarco,²⁶ S.L. Careccia,²⁹ D.S. Carman,²⁸ B. Carnahan,⁵ S. Chen,¹² P.L. Cole,^{35,16} A. Coleman,^{39,†} P. Coltharp,¹² D. Cords,^{35,‡} P. Corvisiero,¹⁸ D. Crabb,³⁸ H. Crannell,⁵ J.P. Cummings,³¹ E. De Sanctis,¹⁷ R. DeVita,¹⁸ P.V. Degtyarenko,³⁵ H. Denizli,³⁰ L. Dennis,¹² A. Deur,³⁵ K.V. Dharmawardane,²⁹ K.S. Dhuga,¹³ C. Djalali,³⁴ G.E. Dodge,²⁹ J. Donnelly,¹⁴ D. Doughty,^{7,35} P. Dragovitsch,¹² S. Dytman,³⁰ O.P. Dzyubak,³⁴ H. Egiyan,^{26,39,35} K.S. Egiyan,⁴⁰ L. Elouadrhiri,^{7,35} A. Empl,³¹ P. Eugenio,¹² R. Fatemi,³⁸ G. Fedotov,²⁵ G. Feldman,¹³ R.J. Feuerbach,⁴ T.A. Forest,²⁹ H. Funsten,³⁹ M. Garçon,⁶ G. Gavalian,^{26,40,29} G.P. Gilfoyle,³³ K.L. Giovanetti,²¹ F.X. Girod,⁶ J.T. Goetz,² R.W. Gothe,³⁴ K.A. Griffioen,³⁹ M. Guidal,¹⁹ M. Guillo,³⁴ N. Guler,²⁹ L. Guo,³⁵ V. Gyurjyan,³⁵ C. Hadjidakis,¹⁹ R.S. Hakobyan,⁵ J. Hardie,^{7,35} D. Heddle,^{7,35} F.W. Hersman,²⁶ K. Hicks,²⁸ I. Hleiqawi,²⁸ M. Holtrop,²⁶ J. Hu,³¹ M. Huertas,³⁴ C.E. Hyde-Wright,²⁹ Y. Ilieva,¹³ D.G. Ireland,¹⁴ B.S. Ishkhanov,²⁵ M.M. Ito,³⁵ D. Jenkins,³⁷ H.S. Jo,¹⁹ K. Joo,^{38,8} H.G. Juengst,^{29,13} J.D. Kellie,¹⁴ M. Khandaker,²⁷ K.Y. Kim,³⁰ K. Kim,²² W. Kim,²² A. Klein,²⁹ F.J. Klein,^{35,5} A.V. Klimenko,²⁹ M. Klusman,³¹ M. Kossov,²⁰ L.H. Kramer,^{11,35} V. Kubarovsky,³¹ J. Kuhn,⁴ S.E. Kuhn,²⁹ J. Lachniet,⁴ J.M. Laget,^{6,35} J. Langheinrich,³⁴ D. Lawrence,²⁴ T. Lee,²⁶ A.C.S. Lima,¹³ K. Livingston,¹⁴ K. Lukashin,^{5,35} J.J. Manak,³⁵ C. Marchand,⁶ L.C. Maximon,¹³ S. McAleer,¹² B. McKinnon,¹⁴ J.W.C. McNabb,⁴ B.A. Mecking,³⁵ M.D. Mestayer,³⁵ C.A. Meyer,⁴ T. Mibe,²⁸ K. Mikhailov,²⁰ R. Minehart,³⁸ M. Mirazita,¹⁷ R. Miskimen,²⁴ V. Mokeev,²⁵ S.A. Morrow,^{6,19} V. Muccifora,¹⁷ J. Mueller,³⁰ G.S. Mutchler,³² P. Nadel-Turonski,¹³ J. Napolitano,³¹ R. Nasseripour,^{34,11} S. Niccolai,^{13,19} G. Niculescu,²¹ B.B. Niczyporuk,³⁵ R.A. Niyazov,^{29,35} M. Nozar,³⁵ G.V. O'Rielly,¹³ M. Osipenko,^{18,25} A.I. Ostrovidov,¹² K. Park,²² C. Paterson,¹⁴ S.A. Philips,^{13,§} J. Pierce,³⁸ N. Pivnyuk,²⁰ D. Pocanic,³⁸ O. Pogorelko,²⁰ S. Pozdniakov,²⁰ B.M. Preedom,³⁴ J.W. Price,^{2,3} Y. Prok,^{23,35} D. Protopopescu,¹⁴ L.M. Qin,²⁹ B.A. Raue,^{11,35} G. Riccardi,¹² G. Ricco,¹⁸ M. Ripani,¹⁸ F. Ronchetti,¹⁷ G. Rosner,¹⁴ P. Rossi,¹⁷ D. Rowntree,²³ P.D. Rubin,³³ F. Sabatié,^{29,6} C. Salgado,²⁷ J.P. Santoro,^{5,35} V. Sapunenko,^{18,35} R.A. Schumacher,⁴ V.S. Serov,²⁰ A. Shafi,¹³ Y.G. Sharabian,^{40,35} J. Shaw,²⁴ S. Simionatto,¹³ A.V. Skabelin,²³ E.S. Smith,³⁵ L.C. Smith,³⁸ D.I. Sober,⁵ M. Spraker,¹⁴ A. Stavinsky,²⁰ S.S. Stepanyan,²² S. Stepanyan,^{35,40} B.E. Stokes,¹² P. Stoler,³¹ I.I. Strakovsky,¹³ S. Strauch,^{13,34} M. Taiuti,¹⁸ S. Taylor,³² D.J. Tedeschi,³⁴ U. Thoma,^{15,35} R. Thompson,³⁰ A. Tkabladze,¹³ S. Tkachenko,²⁹ C. Tur,³⁴ M. Ungaro,^{31,8} M.F. Vineyard,^{36,33} A.V. Vlassov,²⁰ K. Wang,³⁸ L.B. Weinstein,²⁹ H. Weller,⁹ D.P. Weygand,³⁵ M. Williams,⁴ E. Wolin,³⁵ M.H. Wood,^{24,34} A. Yegneswaran,³⁵ J. Yun,²⁹ L. Zana,²⁶ and J. Zhang²⁹

(The CLAS Collaboration)

¹Arizona State University, Tempe, Arizona 85287-1504

²University of California at Los Angeles, Los Angeles, California 90095-1547

³California State University, Dominguez Hills, Carson, California 90747-0005

⁴Carnegie Mellon University, Pittsburgh, Pennsylvania 15213

⁵Catholic University of America, Washington, D.C. 20064

⁶CEA-Saclay, Service de Physique Nucléaire, F91191 Gif-sur-Yvette, Cedex, France

⁷Christopher Newport University, Newport News, Virginia 23606

⁸University of Connecticut, Storrs, Connecticut 06269

⁹Duke University, Durham, North Carolina 27708-0305

¹⁰Edinburgh University, Edinburgh EH9 3JZ, United Kingdom

¹¹Florida International University, Miami, Florida 33199

¹²Florida State University, Tallahassee, Florida 32306

¹³The George Washington University, Washington, DC 20052

¹⁴University of Glasgow, Glasgow G12 8QQ, United Kingdom

¹⁵Physikalisches Institut der Universität Giessen, 35392 Giessen, Germany

¹⁶Idaho State University, Pocatello, Idaho 83209

¹⁷INFN, Laboratori Nazionali di Frascati, 00044, Frascati, Italy

¹⁸INFN, Sezione di Genova, 16146 Genova, Italy

¹⁹Institut de Physique Nucleaire ORSAY, Orsay, France

²⁰Institute of Theoretical and Experimental Physics, Moscow, 117259, Russia

- ²¹James Madison University, Harrisonburg, Virginia 22807
²²Kyungpook National University, Daegu 702-701, South Korea
²³Massachusetts Institute of Technology, Cambridge, Massachusetts 02139-4307
²⁴University of Massachusetts, Amherst, Massachusetts 01003
²⁵Moscow State University, General Nuclear Physics Institute, 119899 Moscow, Russia
²⁶University of New Hampshire, Durham, New Hampshire 03824-3568
²⁷Norfolk State University, Norfolk, Virginia 23504
²⁸Ohio University, Athens, Ohio 45701
²⁹Old Dominion University, Norfolk, Virginia 23529
³⁰University of Pittsburgh, Pittsburgh, Pennsylvania 15260
³¹Rensselaer Polytechnic Institute, Troy, New York 12180-3590
³²Rice University, Houston, Texas 77005-1892
³³University of Richmond, Richmond, Virginia 23173
³⁴University of South Carolina, Columbia, South Carolina 29208
³⁵Thomas Jefferson National Accelerator Facility, Newport News, Virginia 23606
³⁶Union College, Schenectady, NY 12308
³⁷Virginia Polytechnic Institute and State University, Blacksburg, Virginia 24061-0435
³⁸University of Virginia, Charlottesville, Virginia 22901
³⁹College of William and Mary, Williamsburg, Virginia 23187-8795
⁴⁰Yerevan Physics Institute, 375036 Yerevan, Armenia
- (Dated: June 26, 2018)

Differential cross sections for the reaction $\gamma p \rightarrow \eta' p$ have been measured with the CLAS spectrometer and a tagged photon beam with energies from 1.527 to 2.227 GeV. The results reported here possess much greater accuracy than previous measurements. Analyses of these data suggest for the first time the coupling of the $\eta' N$ channel to both the $S_{11}(1535)$ and $P_{11}(1710)$ resonances, known to couple strongly to the ηN channel in photoproduction on the proton, and the importance of $J = 3/2$ resonances in the process.

PACS numbers: 13.60.Le, 14.20.Gk

Understanding the structure of the proton is challenging due to the great complexity of this strongly interacting multi-quark system [1]. Of particular utility in investigating nucleon structure are those production mechanisms and observables that help isolate individual excited states of the nucleon and determine the importance of specific contributions. Since the electromagnetic interaction is well understood, photoproduction offers one of the more powerful methods for studying the nucleon. Since the η and η' mesons have isospin 0, ηN and $\eta' N$ final states can only originate (in one-step processes) from isospin $I = 1/2$ intermediate states. Therefore, the reactions $\gamma p \rightarrow \eta p$ and $\gamma p \rightarrow \eta' p$ isolate $I = 1/2$ resonances, thereby providing an “isospin filter” for the spectrum of broad, overlapping nucleon resonances, a useful simplification for theoretical efforts to predict the large number of excited nucleon states.

Thus, photoproduction of the η' meson from the proton is an excellent tool for clarifying the details of the nucleon resonance spectrum. However, existing data for the $\gamma p \rightarrow \eta' p$ reaction come from only a few exclusive or semi-exclusive measurements due to the limitations of experimental facilities. While previous experiments [2, 3, 4] detected fewer than 300 η' events, in the measurements described here, over 2×10^5 η' photoproduction events were detected and used to extract differential cross sections.

The differential cross sections for the reaction $\gamma p \rightarrow \eta' p$

were measured with the CEBAF Large Acceptance Spectrometer (CLAS) [5] and the bremsstrahlung photon tagging facility [6] at the Thomas Jefferson National Accelerator Facility. The cross sections were part of a program of meson production measurements using the same CLAS, tagger, and target configuration. Tagged photons, with energies E_γ between 0.49 and 2.96 GeV, were incident on an 18-cm-long liquid hydrogen target placed at the center of CLAS. (The threshold for η' photoproduction on the proton is $E_\gamma = 1.447$ GeV.) The event trigger required the coincidence of a post-bremsstrahlung electron passing through the focal plane of the photon tagger and at least one charged particle detected in CLAS. Tracking of the charged particles through the magnetic field within CLAS by drift chambers provided determination of their charge, momentum and scattering angle. This information, together with the particle velocity measured by the time-of-flight scintillators, provided particle identification for each particle detected in CLAS and its corresponding momentum four-vector. Particle identification was generally unambiguous; in the case of proton identification, the fraction of particles misidentified as protons made up a background of less than 2×10^{-3} .

The $\gamma p \rightarrow pX$ missing mass was used to identify photoproduced mesons through detection of the proton recoiling into the CLAS from the cryogenic target. As seen in the missing mass spectrum in Fig. 1, the resolution obtained is sufficient for clear identification of the pho-

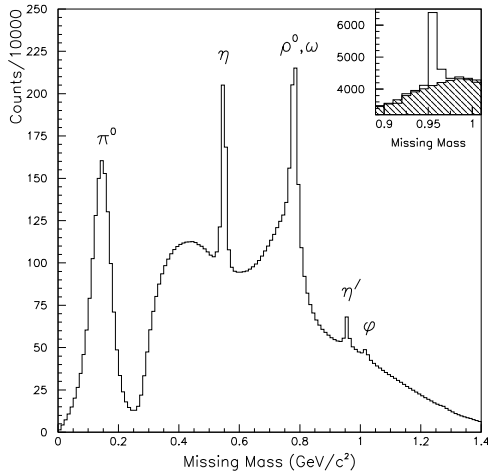


FIG. 1: Missing mass spectrum for $\gamma p \rightarrow pX$ integrated over all photon energies and angles. Inset: Missing mass spectrum binned in photon energy (1.728 ± 0.025 GeV) and angle ($-0.2 \leq \cos \vartheta'_{c.m.} \leq 0.0$), illustrating a typical bin. The shaded area shows the multi-pion background discussed in the text.

toproduced π^0 , η , $\rho + \omega$, η' , and φ mesons, the latter four peaks situated atop a multi-pion background. The missing mass spectrum was binned in center-of-mass scattering angle and photon energy to extract meson yields for each angle/energy bin. The CLAS acceptance limited the measurement of the $\gamma p \rightarrow \eta' p$ reaction to photon energies above 1.527 GeV ($W = 1.94$ GeV) and η' center-of-mass scattering angles $\vartheta'_{c.m.}$ in the range $-0.8 \leq \cos \vartheta'_{c.m.} \leq 0.8$. For the η' measurements reported here, a total of 15 non-overlapping bins in incident photon energy E_γ were used, each about 50 MeV wide. (For convenience, the photon energy bins are labeled by the energy of the centroid of the bin.) The photon energies ranged from bins centered on E_γ from 1.527 up to 2.227 GeV, corresponding to center-of-mass energies W from 1.94 to 2.25 GeV. Above this energy range, the yield for η' photoproduction was too low to permit the extraction of reliable cross sections. The background subtraction (as exemplified in the inset in Fig. 1) assumed a mixture of two-, three-, and four-pion contributions, along with contributions from the ρ^0 .

The proton detection efficiency for CLAS was measured empirically [7, 8] using the reaction $\gamma p \rightarrow p\pi^+\pi^-$. Both pions were required to be detected in the event and both must have been produced by the same photon from the bremsstrahlung beam. A missing mass reconstruction from the kinematical information for the two pions was performed to determine if a proton should have been seen in the CLAS in a particular phase-space volume. The presence or absence of a proton yielded an empirical measure of the momentum-dependent proton detection efficiency for that volume. Efficiency uncertainties for

η' photoproduction, dominated by the statistical uncertainty in the number of protons scattered and detected, were determined for each bin, and ranged from $\sim 1\%$ at the lowest energies to $\sim 2\%$ at the highest energies.

The results reported here represent the first measurements for η' photoproduction utilizing an *absolute* measurement of the photon flux [9]. The photon flux for the entire tagger photon energy range was determined by measuring the rate of scattered electrons detected in each counter of the focal plane of the bremsstrahlung photon tagger by sampling focal plane hits not in coincidence with CLAS. The detection rate for the scattered electrons was integrated over the livetime of the experiment and converted to the total number of photons on target for each counter of the tagger focal plane. The tagging efficiency was measured in dedicated runs with a Total Absorption Counter (TAC) [6], which directly counted all photons in the beam [9].

Ideally, one would use a well-known reaction in the energy range used for these measurements to confirm the validity of the photon flux measurement technique and to estimate the uncertainties in the photon flux normalization. However, no large database exists for any photoproduction reaction over the range of photon energies for which we report η' cross sections here. As an alternative, the pion photoproduction database is quite extensive. The SAID parameterization [10] provides a very good description of that database. The SAID analysis incorporates many observables for all channels of pion photoproduction. The existing π^0 photoproduction cross section database below 1.5 GeV is quite dense. (The data below 1.5 GeV make up 95% of the published measurements on π^0 photoproduction on the proton.) The SAID solution (SM02) is in very good agreement with those existing data. Thus, SAID can be assumed to provide the correct energy and angular dependence for the π^0 photoproduction cross section in that energy range within its estimated normalization uncertainty of 2%. The existing data above 1.5 GeV are much more scarce and have significantly larger uncertainties. Therefore, we have used that parametrization to ascertain the validity of the procedures used here by comparing that SAID parametrization to π^0 photoproduction cross sections (for E_γ from 0.675 to 1.525 GeV) extracted from data taken simultaneously with the η' measurements reported here (for E_γ from 1.527 to 2.227 GeV), using the same absolute normalization techniques for both reactions [11].

In order to determine the π^0 cross sections for this experiment over the photon energy range from 0.675 to 1.525 GeV, the empirically measured proton detection efficiency for CLAS had to be supplemented by a Monte-Carlo estimate of the detection efficiency for protons from π^0 photoproduction because the phase space occupation of protons for the $\gamma p \rightarrow p\pi^+\pi^-$ reaction becomes sparse at higher energies when rebinned for $\gamma p \rightarrow p\pi^0$ efficiencies. Agreement between the empirical and Monte-

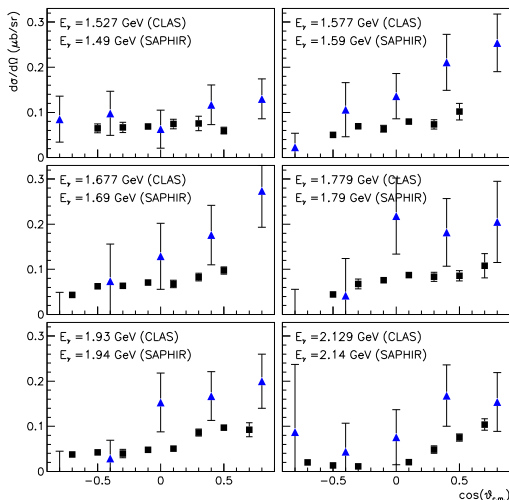


FIG. 2: Differential cross sections for η' photoproduction on the proton (black squares). Other results from SAPHIR [4] (blue triangles) are shown for comparison. Error bars shown include systematic and statistical uncertainties.

Carlo methods, where sufficient statistics made comparison possible, was within 3%.

For E_γ from 0.675 to 1.525 GeV and the range of $\cos(\vartheta_{\text{c.m.}}^{\pi^0})$ used here, our entire set of π^0 differential cross sections, comprised of 19 energy bins each with 12 bins in $\cos(\vartheta_{\text{c.m.}}^{\pi^0})$ (228 points, in total) was easily fit by the SAID parametrization with a single overall constant factor $N = 1.02$ ($\chi_{\text{reduced}}^2 = 1.3$). *This overall agreement throughout the energy range implies that the absolute normalization technique is sound, and additionally indicates the detector acceptance also is well-determined.*

To estimate the uncertainty in the photon flux measurement, a more refined fit of our measured differential cross sections for π^0 photoproduction for *each* photon energy bin to the SAID parametrization was performed, determining a single overall constant factor N_E for *each* photon energy bin. For $E_\gamma = 0.675$ to 1.525 GeV, these $N_E(E_\gamma)$ values were produced, binned into a histogram, and fit with a simple Gaussian. The centroid of the fit to $N_E(E_\gamma)$ was 1.02, as before. The standard deviation $\sigma(N_E(E_\gamma))$ of the $N_E(E_\gamma)$ values was 4%. We conservatively estimate the absolute normalization systematic uncertainty to be about 5%.

The differential cross sections for η' photoproduction obtained are shown in Figs. 2 and 3. In general, the angular distributions, while flat at threshold, show a continuing increase in slope at forward angles with increasing photon energy. At the highest energies, growth at backward angles is also seen. These general features are suggestive of coupling to an s-channel resonance near threshold, with increasing contributions of t- and u-channel exchange as the energy above threshold increases. The SAPHIR measurements [4] are shown for comparison in

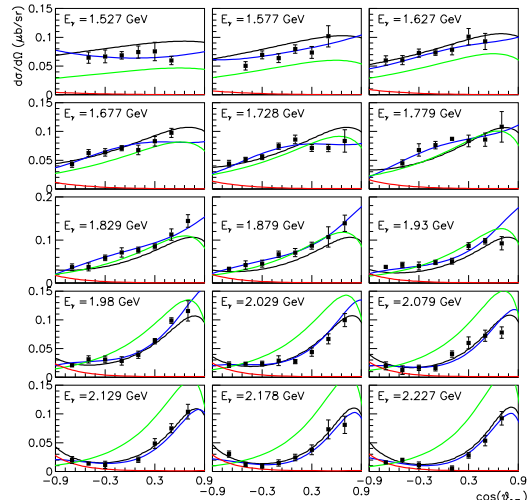


FIG. 3: Differential cross sections for η' photoproduction on the proton. Also shown are results from Nakayama and Haberzettl [12] (Red lines: u -channel contributions. Green lines: t -channel contributions. Blue lines: Sum of all s -, t -, and u -channel contributions), and a model (black lines) inspired by A. Sibirtsev *et al.* [19], as discussed in the text. Error bars shown include systematic and statistical uncertainties.

Fig. 2. The CLAS data, with much smaller error bars and smaller photon energy bins (SAPHIR has energy bins of 100 MeV for energies below 1.84 GeV and 200 MeV wide bins above), generally agree with the SAPHIR results within the very large error bars of the latter, but the CLAS values are nonetheless systematically lower. The excellent agreement noted above between the SAID parametrization and the π^0 photoproduction cross sections measured here, using the same normalization techniques as used for these η' cross sections, strongly suggests the absolute normalization determined here is correct.

Included in Fig. 3 are the results (shown as red, green, and blue lines) representing a consistent analysis of the reactions $\gamma p \rightarrow p\eta'$ and $pp \rightarrow pp\eta'$ by Nakayama and Haberzettl (NH) [12]. The NH analysis is based upon a relativistic meson-exchange model of hadronic interactions including coupled-production mechanisms. We have also performed calculations (black lines) using a relativistic meson-exchange model by A. Sibirtsev *et al.* [19] as a recipe. For both models, allowed processes include s -, t -, and u -channel contributions. The intermediate mesons in the t -channel exchanges are the ω and ρ^0 in both cases. Both models here also included the $S_{11}(1535)$ and $P_{11}(1710)$ resonances ($J = 1/2$), which are known to decay strongly to the ηN channel [13]. The NH model also includes two additional S_{11} and two additional P_{11} resonances, albeit with relatively small couplings. In contrast to the fit of the SAPHIR data in Ref. [4], the

present adaptation of the NH model to our data now also requires $J = 3/2$ resonances [$P_{13}(1940)$, $D_{13}(1780)$, and $D_{13}(2090)$]. Since the NH model fits the data better than our calculations, the inclusion of these additional $J = 3/2$ resonances appears to be beneficial.

A comparison of the predictions of these two different approaches can provide insight into which physical contributions are most successful at explaining features of the observed cross sections. The forward peaking of the cross sections at the highest energies is dominated by t -channel exchange. Addition of the $S_{11}(1535)$ state contributes mainly to the overall initial rise and fall of the total cross sections below 1.7 GeV. We note that this is the first time that $S_{11}(1535)$ and $P_{11}(1710)$ resonances, known to strongly couple to the ηN channel in photoproduction, have been used in fits as contributions to the $\eta' N$ photoproduction channel. The $J = 3/2$ resonances included by NH are especially useful in obtaining the correct shape of the differential cross sections for the energies from 1.728 to 1.879 GeV. The u -channel exchange causes the backward-angle enhancement seen around 2 GeV and above. (The general behavior of individual t - and u -channel contributions can be seen in Fig. 3 and Ref. [14].)

Since the η' meson is the only flavor singlet of the fundamental pseudoscalar meson nonet, studies of the reaction can also help yield information on the role of glue states in excitations of the nucleon. The flavor-singlet axial charge of the nucleon ($G_A(0)$) is related to the η' -nucleon-nucleon and gluon-nucleon-nucleon coupling constants ($g_{\eta' NN}$ and $g_{GNN}(0)$, respectively) through the flavor-singlet Goldberger-Treiman relation [15]:

$$2m_N G_A(0) = F g_{\eta' NN} - \frac{F^2 m_{\eta'}^2}{N_F} g_{GNN}(0), \quad (1)$$

where m_N is the mass of the nucleon, $m_{\eta'}$ is the η' mass, F is an invariant decay constant that reduces to F_π (pion decay constant) if the $U(1)_A$ anomaly were turned off [16], and N_F equals the number of flavors. When first measured [17], the singlet axial charge was found to have a value of $G_A(0) = 0.20 \pm 0.35$. (A more recent calculation [18] gives $G_A(0) = 0.213 \pm 0.138$.) At that time, the importance of the second term in Eq. 1 was unappreciated, and this low value of $G_A(0)$ was surprising: Since $g_{\eta' NN}$ is considered to be correlated with the fraction of the nucleon spin carried by its constituent quarks [19], that fraction would then be consistent with zero. Thus, neglecting the gluonic portion of Eq. 1 was one of the causes of the so-called “spin crisis.” However, by including the gluonic degrees of freedom in Eq. 1, the value of $g_{\eta' NN}$ can be large, provided that it is nearly canceled by $g_{GNN}(0)$. This equation then can be used to indirectly determine the gluonic coupling to the nucleon given a value of $g_{\eta' NN}$.

The observed u -channel contribution seen here allows the $g_{\eta' NN}$ coupling to be extracted (albeit in a model-

dependent way). The value of $g_{\eta' NN}$ found from the particular NH fit shown here is 1.33, whereas our results using the model of Ref. [19] provides 1.46. Since differential cross sections alone do not provide sufficient constraints to these models, these $g_{\eta' NN}$ values should be taken with caution. Nonetheless, both values of $g_{\eta' NN}$ are consistent with the analysis of Ref. [16] which gives 1.4 ± 1.1 . Moreover, even though the uncertainty in $g_{\eta' NN}$ precludes a definitive statement about the value of $g_{GNN}(0)$, Eq. 1 can be carried out taking $N_F = 3$, $F = F_\pi = 0.131$ GeV, $g_{\eta' NN} = 1.4$, and $G_A(0) = 2.13$, yielding the result that $g_{GNN}(0) = 41$ GeV⁻³.

In conclusion, the differential cross sections presented here are the first high-quality data for the $\gamma p \rightarrow \eta' p$ reaction. An analysis of the data with two different models of the process suggests for the first time contributions from both the $S_{11}(1535)$ and $P_{11}(1710)$ nucleon resonances to the $\eta' N$ channel in photoproduction, the two resonances previously identified as strongly coupling to the ηN channel [13]. Using two different theoretical descriptions of the data, these cross sections suggest a value for the η' -nucleon-nucleon coupling constant $g_{\eta' NN}$ of 1.3-1.5, consistent with previous theoretical estimates of this quantity. These data should continue to prove quite useful in guiding future experimental and theoretical investigations of the structure of the nucleon.

The authors gratefully acknowledge the Jefferson Lab Accelerator Division staff. We thank W. Kaufmann, H. Haberzettl and K. Nakayama for useful discussions and assistance. This work was supported by the National Science Foundation, the Department of Energy (DOE), the Deutsche Forschungsgemeinschaft (through an Emmy Noether grant to U.T.), the French Centre National de la Recherche Scientifique and Commissariat à l’Energie Atomique, the Italian Istituto Nazionale di Fisica Nucleare, and the Korean Science and Engineering Foundation. The Southeastern Universities Research Association operates Jefferson Lab for DOE under contract DE-AC05-84ER40150.

* Present address: Sakarya University, Sakarya, Turkey

† Present address: Systems Planning and Analysis, Alexandria, Virginia 22311

‡ Deceased.

§ Present address: Cabarra Industries, Meriden, Connecticut 06457

- [1] See, e.g., S. Capstick and W. Roberts, *Prog. in Part. and Nucl. Phys.* **45**, S241 (2000).
 [2] ABBHHM Collaboration, *Phys. Rev.* **175**, 1669 (1968).
 [3] AHHM Collaboration, *Nucl. Phys. B* **108**, 45 (1976).
 [4] R. Plötzke *et al.*, *Phys. Lett. B* **444**, 555 (1998).
 [5] B. Mecking *et al.*, *Nucl. Instr. Meth.* **A** 503, 513 (2003).
 [6] D. Sober *et al.*, *Nucl. Instr. Meth.* **A** 440, 263 (2000).
 [7] M. Dugger, Ph.D. dissertation, Arizona State University (unpublished, 2001).

- [8] T. Auger, Ph.D. dissertation, Université de Paris (unpublished, 1999).
- [9] J. Ball and E. Pasyuk, CLAS note 2005-002 (2005) http://www.jlab.org/Hall-B/notes/clas_notes05/2005-002.pdf
- [10] R. A. Arndt, W. J. Briscoe, I. I. Strakovsky, and R. L. Workman, Phys. Rev. C **66**, 055213 (2002); R. A. Arndt, I. I. Strakovsky, R. L. Workman, and M. M. Pavan, Phys. Rev. C **52**, 2120 (1995).
- [11] M. Dugger, *et al.*, The results for π^0 photoproduction will be reported in a forthcoming publication.
- [12] K. Nakayama, and H. Haberzettl, private communication. The results shown here are based on an extended version of the model given in [14].
- [13] S. Eidelman *et al.*, Phys. Lett. B **592**, 1 (2004).
- [14] K. Nakayama and H. Haberzettl, Phys. Rev. C **69**, 065212 (2004).
- [15] G.M. Shore, G. Veneziano, Nucl. Phys. **B381**, 23 (1992)
- [16] T. Feldmann, Int. J. Mod. Phys. A **15** 159 (2000); also available as hep-ph/9907491.
- [17] J. Ashman *et al.*, Nucl. Phys. B **328**, 1 (1989).
- [18] M. Hirai, S. Kumano, N. Saito, Phys. Rev. D **69** 054021 (2004); also available as hep-ph/0312112.
- [19] A. Sibirtsev, Ch. Elster, S. Krewald, and J. Speth, AIP Conf. Proc. **717**, 837 (2004); A. Sibirtsev, Ch. Elster, S. Krewald, and J. Speth, nucl-th/0303044.